

Effective Inflow Conditions for Turbulence Models in Aerodynamic Calculations

Philippe R. Spalart*

Boeing Commercial Airplanes, Seattle, Washington 98124

and

Christopher L. Rumsey†

NASA Langley Research Center, Hampton, Virginia 23681-2199

DOI: 10.2514/1.29373

The selection of inflow values for one- and two-equation turbulence models at boundaries far upstream of an aircraft is considered. Inflow values are distinguished from the ambient values near the body, which may be much smaller because the long approach can allow a deep decay. Ambient values should be selected first, and inflow values that will lead to them after the decay should be second; this is not always possible, especially for the time scale. The decay of turbulence in two-equation models during the approach to the aircraft is shown; in computational fluid dynamics practice, the time scale has often been set too short for this decay to be calculated accurately on typical grids. A simple remedy for both issues is to arrest decay below the chosen ambient values, either by imposing floor values, or preferably by adding weak source terms. A physical justification for overriding the equations in this manner is proposed. Selecting laminar ambient values is easy if the boundary layers are to be tripped, but it is common to seek ambient values that will cause immediate transition in shear layers. This opens up a wide range of values, and selection criteria are discussed. The turbulent Reynolds number, or ratio of eddy viscosity to laminar viscosity has a huge dynamic range that makes it unwieldy; it has been widely misused, particularly by setting upper limits on it. The value of the complete turbulent kinetic energy in a wind tunnel or the atmosphere is also dubious as an input to the model, because its spectrum contains length scales irrelevant to the turbulence in the boundary and shear layers. Concretely, the ambient eddy viscosity must be small enough to preserve potential cores in small geometry features such as flap gaps. The ambient-frequency scale should also be small enough, compared with shear rates in the boundary layer. Specific ranges of values are recommended and demonstrated for airfoil flows.

Nomenclature

a_1	= constant in a turbulence model
$C_{\varepsilon 1}, C_{\varepsilon 2}$	= coefficients in a turbulence model
C_μ	= coefficient in a turbulence model
c	= airfoil chord
c_{i3}, c_{i4}	= constants in a turbulence model
c_{w1}, c_{w3}	= constants in a turbulence model
d	= gap distance between airfoil elements
F_1, F_2	= functions in a turbulence model
k	= turbulence kinetic energy
L	= length scale
\mathcal{P}	= turbulence production
Re	= Reynolds number
Re_t	= turbulent Reynolds number
r	= radius
Tu	= turbulence intensity
t	= time
U	= velocity
x	= coordinate distance, vector, or distance
β, β^*	= coefficients in a turbulence model
γ	= constant in a turbulence model
δ	= boundary-layer thickness
ε	= turbulent dissipation
μ_t	= turbulent eddy viscosity

ν	= kinematic viscosity
$\tilde{\nu}$	= turbulence variable in the Spalart–Allmaras turbulence model
ν_t	= turbulent kinematic viscosity
$\sigma_k, \sigma_\varepsilon$	= constants in a turbulence model
$\sigma_\omega, \sigma_{\omega 2}$	= constants in a turbulence model
Ω	= magnitude of vorticity
ω	= dissipation per unit turbulence kinetic energy

Subscripts

amb	= ambient
c	= based on airfoil chord
floor	= floor value
FS	= freestream or inflow
j	= index direction
L	= based on length scale L
x	= derivative with respect to x
∞	= at infinity or freestream

I. Introduction

TURBULENCE models based on transport equations are now omnipresent, but the computational fluid dynamics (CFD) community's knowledge of appropriate boundary conditions for the turbulence variables at distant boundaries is incomplete. There is much room for clarity and helpfulness in some of the original turbulence-model papers and in the manuals and graphical user interfaces of widely used codes. Solid physical interpretations of the values taken by the primary variables and the eddy viscosity derived from them are needed. A contributing factor is the large dynamic range of the variables; for instance, the eddy viscosity may logically be compared with the molecular viscosity or with the product of velocity and length of the aircraft, and these two numbers may differ by a factor of 10^8 (i.e., the aircraft Reynolds number). The choice between these two scales is a source of confusion and interferes with

Received 19 December 2006; revision received 18 May 2007; accepted for publication 4 June 2007. Copyright © 2007 by the American Institute of Aeronautics and Astronautics, Inc. All rights reserved. Copies of this paper may be made for personal or internal use, on condition that the copier pay the \$10.00 per-copy fee to the Copyright Clearance Center, Inc., 222 Rosewood Drive, Danvers, MA 01923; include the code 0001-1452/07 \$10.00 in correspondence with the CCC.

*Boeing Senior Technical Fellow, Mail Stop 67-LM, P.O. Box 3707; philippe.r.spalart@boeing.com. Member AIAA.

†Senior Research Scientist, Computational Aerosciences Branch, Mail Stop 128. Member AIAA.

the establishment of guidelines. This situation creates pitfalls, among which are failures to produce turbulence where intended by the user [1] and excessive eddy-viscosity values in regions that have not produced turbulence and should remain irrotational. These pitfalls, which are preventable, may well go undetected when the models are treated as black boxes. Our purpose here is to recommend sound prevention measures. By *effective*, we mean boundary-condition practices that do not add much to the users' burden and that ensure a low sensitivity of the results to trivial parameters. For instance, it would be unacceptable to get different results from a computation with one domain 50 chords in radius and another domain 60 chords in radius. Progress in science and engineering depends on repeatability and on building an experience base that is genuine.

It may help to start from the *ideal situation* that a trusting CFD user would expect. The incoming stream has well-defined turbulence kinetic energy and dissipation, k and ε , and eddy viscosity derived from them, $v_t = C_\mu k^2/\varepsilon$ (for a physical reason and not only dimensional analysis). These quantities correctly respond to velocity gradients while approaching the aircraft and couple meaningfully with the boundary-layer turbulence. It is simply a matter of knowing k and ε far upstream, preferably from measurements. These values are realistic.

This vision fails, primarily because describing all of turbulence with two numbers is insufficient. Here, we disregard internal flows (in particular, gas-turbine applications, for which the coupling with ambient turbulence is stronger) and address only external aircraft flows. In the atmospheric boundary layer, modeled with Reynolds-averaged Navier-Stokes (RANS) equations, the eddy viscosity on a windy day can well take values such as $50 \text{ m}^2/\text{s}$, and the chord Reynolds number of a large airplane based on this eddy viscosity would be near five. This is untenable, of course. The reason is that the eddies that may couple with the boundary layer have sizes on the order of 1 cm, rather than 100 m, so that only a tiny fraction of the atmospheric k is relevant and the much larger eddies are felt as unsteadiness (the analogous estimates in a wind tunnel are not as immensely different, but the physical consequences are the same). This relevant fraction is deduced from the atmospheric dissipation rate and a length scale, much better than from the atmospheric k , and it is not sharply defined. Moreover, it has no reason to obey the decay equations used to calibrate two-equation models in isotropic turbulence. In reality, the kinetic energy relevant to the aircraft flow varies very little over the size of the CFD domain. This fact is in strong conflict with common practices in CFD, because inflow values of ε/k near U_∞/c are routinely used, where U_∞ is the speed of the aircraft and c the wing chord. Over an approach to the aircraft of length $50c$, k then drops by a factor of about 75, if the solution is accurate according to the decay equations. This is obviously unrealistic behavior, accepted in an attempt to obtain the desired behavior in the boundary layers.

Similarly, unreasonably high inflow values of k have been occasionally used, up to freestream turbulence levels of over 5%. Furthermore, only the eddy viscosity has a strong influence on the flowfield, at least at moderate Mach numbers; k and ε separately do not (second-moment closures would be different). In fact, most CFD users are only interested in whether the solution is laminar or turbulent, and of those, the vast majority have no interest in laminar regions. Fully turbulent (FT) behavior is safer and gives better convergence and can be viewed as the standard mode of use of RANS models today, to the dismay of some observers. A contributing factor is some unreliability in achieving transition, even if the model allows it at all. For example, the Spalart-Allmaras model [2] is equipped with trip terms in its official version, but the tripping function is not trouble-free. It is costly in a general 3-D grid, and sometimes transition fails, or else moves upstream of the trip because of poor resolution unless the grid is adapted. Tripping is offered in very few codes, although there is certainly a desire for turbulence-model developers to improve capability in this area.

In addition to being unrealistic, the precipitous decay associated with such inflow values is not calculated accurately. A typical grid spacing near the inflow boundary is larger than c , which is too large to resolve a decay at a rate $1/c$. This is observed in otherwise fully

normal CFD solutions; the decay is grossly underestimated and grid-dependent, as shown later. The boundary-layer turbulence responds only to what we will call the ambient values of the turbulence variables: those in the vicinity of the aircraft. Thus, for example, grid-dependent ambient values can have an influence on the location in the boundary layer in which the model trips to turbulence. Because small variations in transition location do not typically have a glaring impact on the global results, this problem is largely out of sight for the user. However, the situation is problematic from the point of view of consistency.

Different CFD codes handle the issue of freestream turbulence differently. Many assign default values and allow the user to override those if desired. However, there is usually very little guidance given as to how different choices affect the decay rates and the resulting levels that are actually seen near the body. Some codes (such as the CFD++ code [3]) allow the user to disable the decay in some regions, which are manually defined with controls such as x_{\min} and x_{\max} . This manner of control is not very practical for real-life geometries, although placing x_{\max} near the forward end of the aircraft is easy and does lessen the decay problem. Other groups prevent the decay by imposing floor values: the turbulence variables are limited by nonzero minimum values. This limiting may conflict with the wall boundary condition for k , but this can be resolved using the SST model's F_1 function [4], for instance. More important is the question of whether violating the celebrated $k-\varepsilon$ equations by imposing floor values can be justified at all; this is taken up later.

In the remainder of the paper, the focus will be on the two-equation $k-\omega$ SST model [4] and the one-equation model of Spalart and Allmaras (S-A) [2], but theoretical aspects of the $k-\varepsilon$ model will also be considered. The equations for free decay are presented first, leading to reverse-engineering inflow values from ambient values; controlled decay is then examined. Then the valid criteria that exist to pick ambient and/or inflow values are discussed. This is followed by examples that support the recommendations made and a summary.

II. Decay Equations and Control

A. Free Decay

Free decay rates of turbulence quantities can be very large and nonphysical when commonly used inflow values are specified. This can be seen from the solution to the $k-\varepsilon$ equations in the approaching flowfield. A typical form of the complete $k-\varepsilon$ equations can be written [5]

$$\frac{Dk}{Dt} = \mathcal{P} - \varepsilon + \frac{\partial}{\partial x_j} \left[\left(v + \frac{v_t}{\sigma_k} \right) \frac{\partial k}{\partial x_j} \right] \quad (1)$$

$$\frac{D\varepsilon}{Dt} = \frac{\varepsilon}{k} (C_{\varepsilon 1} \mathcal{P} - C_{\varepsilon 2} \varepsilon) + \frac{\partial}{\partial x_j} \left[\left(v + \frac{v_t}{\sigma_\varepsilon} \right) \frac{\partial \varepsilon}{\partial x_j} \right] \quad (2)$$

with $v_t = C_\mu k^2/\varepsilon$, and $C_\mu = 0.09$. In the approach to the aircraft, only the destruction terms are active, so that $Uk_x = -\varepsilon$ and $U\varepsilon_x = -C_{\varepsilon 2}\varepsilon^2/k$ to a very good approximation. The solution is simple and linear for k/ε :

$$\frac{k}{\varepsilon} = \left(\frac{k}{\varepsilon} \right)_{FS} + (C_{\varepsilon 2} - 1) \frac{x}{U} \quad (3)$$

where the subscript FS is the freestream, or inflow, and x is the distance from the inflow to the field point. Control over the time scale k/ε through the inflow value is difficult; nothing can prevent it from growing. Typically, $C_{\varepsilon 2} = 1.92$, so that during such a decay, the increase in the time scale is almost equal to the age of the turbulence.

The solutions for k , ε , and v_t are then

$$k = k_{FS} \left[1 + (C_{\varepsilon 2} - 1) \left(\frac{\varepsilon}{k} \right)_{FS} \frac{x}{U} \right]^{\frac{-1}{C_{\varepsilon 2}-1}} \quad (4)$$

$$\varepsilon = \varepsilon_{\text{FS}} \left[1 + (C_{\varepsilon 2} - 1) \left(\frac{\varepsilon}{k} \right)_{\text{FS}} \frac{x}{U} \right]^{\frac{-C_{\varepsilon 2}}{C_{\varepsilon 2} - 1}} \quad (5)$$

$$\nu_t = \nu_{t,\text{FS}} \left[1 + (C_{\varepsilon 2} - 1) \left(\frac{\varepsilon}{k} \right)_{\text{FS}} \frac{x}{U} \right]^{\frac{C_{\varepsilon 2} - 2}{C_{\varepsilon 2} - 1}} \quad (6)$$

It is seen that ν_t decays much more slowly than k and ε : the power is about -0.09 versus -1.1 and -2.1 , respectively. Numerical tests have confirmed this decay, but have also shown that it is calculated accurately from the onset only if ε/k is small enough compared with $U_\infty/\Delta x$, where Δx is the streamwise grid spacing. When Δx is too large to support accurate computations in the far field and the code is robust enough to avoid negative values, the decay simply tends to be delayed. During the approach, both ε/k and $U_\infty/\Delta x$ evolve in the direction needed to improve their ratio, making the resolution easier. This situation remains aesthetically undesirable, and likely to cause jumps during grid sequencing, among other things. It could also disturb the order of accuracy of the solver.

The freestream decay of ω (for the $k-\omega$ model) can be found in a similar fashion. For example, the $k-\omega$ SST model is given by

$$\frac{Dk}{Dt} = \mathcal{P} - \beta^* \omega k + \frac{\partial}{\partial x_j} \left[\left(\nu + \frac{\nu_t}{\sigma_k} \right) \frac{\partial k}{\partial x_j} \right] \quad (7)$$

$$\begin{aligned} \frac{D\omega}{Dt} &= \frac{\gamma}{\mu_t} \mathcal{P} - \beta \omega^2 + \frac{\partial}{\partial x_j} \left[\left(\nu + \frac{\nu_t}{\sigma_\omega} \right) \frac{\partial \omega}{\partial x_j} \right] \\ &\quad + 2(1 - F_1) \frac{1}{\sigma_{\omega 2} \omega} \frac{\partial k}{\partial x_j} \frac{\partial \omega}{\partial x_j} \end{aligned} \quad (8)$$

where $\nu_t = a_1 k / \max(a_1 \omega, \Omega F_2)$, $a_1 = 0.31$, Ω is the magnitude of vorticity, and F_1 and F_2 are blending functions. Here we use the standard convention that $\omega \equiv \varepsilon/(C_\mu k)$. The decay of ω in the freestream is

$$\omega = \omega_{\text{FS}} \left(1 + \frac{\omega_{\text{FS}} \beta x}{U} \right)^{-1} \quad (9)$$

Because β is equivalent to $C_\mu(C_{\varepsilon 2} - 1)$ (with $C_\mu = \beta^* = 0.09$), Eq. (9) is equivalent to Eq. (3), which can also be written as $1/\omega = 1/\omega_{\text{FS}} + C_\mu(C_{\varepsilon 2} - 1)x/U$.

Equations (4–6) and (9) are available to produce the inflow values needed, once ambient values have been chosen. They may also indicate that a set of ambient values is unreachable, with Eq. (3) or Eq. (9) expressing the dominant constraint.

It is clear from these equations that the chosen freestream values of the turbulence quantities have a strong influence on the rate of decay of the turbulence values. Table 1 shows examples of typical freestream levels (for $Re_L = 10 \times 10^6$), along with their decayed levels according to Eqs. (4–6) and (9) at a distance of $x/L = 50$ downstream. The freestream turbulence intensity, in percent, is related to turbulent kinetic energy (TKE) by the relation $Tu = 100\sqrt{2k/(3U^2)}$. The highest value $\omega L/U$ can reach is $1/[50C_\mu(C_{\varepsilon 2} - 1)] = 0.2415$; many of the inflow value sets chosen lead to 0.24, in other words, ω_{FS} was set so high that it lost control of the decayed value. The dramatic decay of k and ε is evident in some of these examples. Taking Tu and $\nu_{t,\text{FS}}$ as the parameters easiest to relate to and varying them independently, this table demonstrates that the higher the freestream turbulence intensity Tu , the more rapid the decay; and the lower the freestream eddy-viscosity level (ν_t), the more rapid the decay. In other words, to achieve reasonable decay rates, one is forced to use either very low levels of freestream Tu , or very high levels of freestream ν_t .

As mentioned earlier, for large decay rates, the coarseness of the grid far from the body may make the solver unable to support an accurate computation and the decay can be grossly underestimated. The behavior of ω for two different freestream turbulence levels is shown in Fig. 1. In particular, it is shown that for the higher

$Tu, \%$	$\nu_{t,\text{FS}}/\nu$	k_{FS}/U^2	$\omega_{\text{FS}} L/U^3$	$\varepsilon_{\text{FS}} L/U^3$	$\nu_t/\nu_{t,\text{FS}}$	k/k_{FS}	$\varepsilon/\varepsilon_{\text{FS}}$	$\omega/\omega_{\text{FS}}$	ν_t/ν	v_t/UL	k/UL^2	$\varepsilon L/U^3$	$\omega L/U$
0.001	0.01	1.5×10^{-10}	2.025×10^{-12}	0.15	0.96	0.59	0.37	0.62	0.0096	9.6×10^{-10}	8.9×10^{-9}	7.5×10^{-13}	0.09
	0.01	1.5×10^{-8}	2.025×10^{-8}	15	0.70	0.11	1.8×10^{-4}	0.016	0.007	$7. \times 10^{-10}$	1.7×10^{-9}	3.6×10^{-12}	0.24
0.1	0.01	1.5×10^{-6}	2.025×10^{-4}	1500	0.47	7.5×10^{-5}	1.2×10^{-8}	1.6×10^{-4}	0.0047	4.7×10^{-10}	1.1×10^{-10}	2.4×10^{-12}	0.24
	0.01	1.5×10^{-4}	2.025×10^0	1.5×10^5	0.31	5.1×10^{-7}	8.1×10^{-13}	1.6×10^{-6}	0.0031	2.1×10^{-10}	7.7×10^{-11}	1.6×10^{-12}	0.24
1.0	0.01	1.5×10^{-6}	2.025×10^{-5}	150	0.57	9.2×10^{-4}	1.5×10^{-6}	1.6×10^{-3}	0.057	5.7×10^{-9}	1.4×10^{-9}	3×10^{-11}	0.24
	0.1	1.5×10^{-6}	2.025×10^{-6}	15	0.70	0.011	1.8×10^{-4}	0.016	0.7	$7. \times 10^{-8}$	1.7×10^{-8}	3.6×10^{-10}	0.24
0.1	1.0	1.5×10^{-6}	2.025×10^{-7}	1.5	0.84	0.12	0.016	0.14	8.4	8.4×10^{-7}	1.8×10^{-9}	3.2×10^{-9}	0.24
	10	1.5×10^{-6}	2.025×10^{-8}	0.15	0.96	0.59	0.37	0.62	96	9.6×10^{-6}	8.9×10^{-7}	7.4×10^{-9}	0.09
0.1	100	1.5×10^{-6}	2.025×10^{-8}										

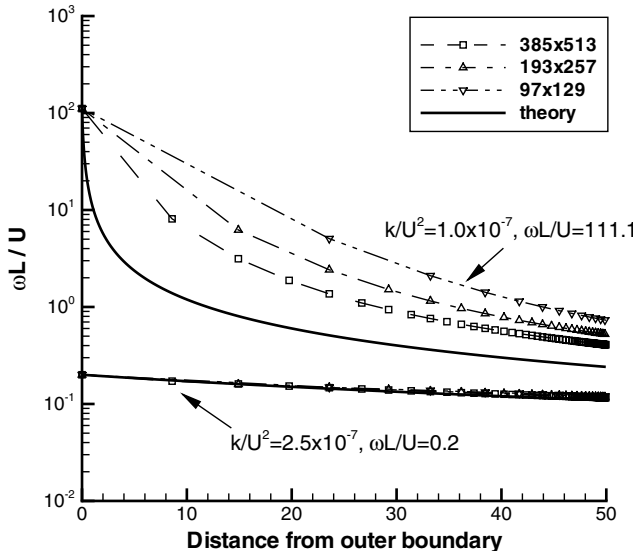


Fig. 1 Evolution of $\omega L/U$ ahead of a NACA 0012 airfoil with $Re_c = 10^7$.

freestream decay conditions, the computed results display a very noticeable grid dependence, only slowly approaching the correct answer as the grid is refined (upper curves). Using significantly lower values for freestream ω , however, the decay rate is dramatically reduced, and CFD predicts the levels with greater precision on all three grids (lower curves).

The equivalent situation for the S-A model is most simple; in the absence of significant destruction term (which is discussed later) and of vorticity (which sets production), the transported variable \tilde{v} and the eddy viscosity ν_t are uniform. Objections have been made to the absence of a destruction term other than wall-related, which may appear unphysical, but here this constitutes a definite advantage. A trivial issue which nevertheless causes confusion is that some user interfaces do not make it clear whether \tilde{v} or ν_t is being set; unfortunately, this is pivotal when the values are of the same order as the molecular viscosity ν . An obliquely related issue is that several groups have used for inflow the value $\tilde{v} = 1.34$, set to give $\nu_t/\nu = 0.009$; this originated in a historical detail of the Baldwin–Barth model [6], using the round number $Re_t = k^2/\nu\epsilon = 0.1$. Unfortunately, this value is not very far from the boundary $\tilde{v}/\nu = \sqrt{\log(c_{13})/c_{14}}$ between those solutions that are attracted by zero once the production term becomes active, due to the f_{12} function in the model, and those that are not [1]. This boundary is at $\tilde{v}/\nu = 0.60$ in the more common version 1a and at $\tilde{v}/\nu = 0.22$ in version 1 of [2]. The f_{12} term can steer \tilde{v} into the basin of attraction, with unpredictable results. Values of \tilde{v}/ν in the 3–5 range are much more reliable than 1.34 when fully turbulent behavior is desired.

B. Controlled Decay

The initial concept for controlled decay (floor values) is simple: k and ϵ (or ω) are not allowed to drop below some preset values. This method is used in the NASA PAB3D code and was suggested to us by Abdol-Hamid et al. [7].

As mentioned already, the conflict with the wall boundary condition $k = 0$ can be removed by conditioning the limiters on F_1 from the SST model, or a similar quantity in other models that detects the interior of the boundary layer. This conditioning should also prevent potential problems for cases with boundary-layer relaminarization. A secondary issue is that preventing the free decay with an override can create the appearance of nonconvergence of the solution, because the residuals will remain nonzero; again, it is remediable and only a reporting issue. We multiplied the destruction term of any variable ϕ by $\max[F_1, H(\phi - \phi_{\text{floor}})]$,[‡] where H is the Heaviside function, and this has worked well in our tests, although

the term can possibly influence the boundary layer in the outer part in which F_1 transitions between 1 and 0.

An alternative to setting floor values is available, as suggested by two of the reviewers, to which we are very grateful. It consists of simply adding source terms ϵ_{amb} and $C_{\epsilon 2}\epsilon_{\text{amb}}^2/k_{\text{amb}}$ to the right-hand side of Eqs. (1) and (2), respectively. This sustaining-term approach enjoys a certain degree of physical support. In addition, it does not need to be disabled near the wall, the way a floor value needs to for k , provided that k_{amb} and ϵ_{amb} are small enough. A function such as F_1 is not needed. A reviewer also suggested disabling the decay control in all shear layers, but the source terms can be set too weak to disturb the shear-flow turbulence.

The philosophical objections against disabling the classical $k-\epsilon$ equations are deeper than the numerical objections, but are surmountable. The small-scale component of a larger turbulence field simply does not decay the way turbulence that has all its energy in the small scales would. Essentially, it has a supply of energy in the Kolmogorov cascade and does not decay unless the energy-supplying eddies do, which is not the case in the atmosphere and is very slight in a wind tunnel over the length of the test section. The TKE contained in scales smaller than l is on the order of $(\epsilon l)^{2/3}$ and the dissipation is ϵ , which is shared by the full turbulence and its small-scale subset. These should give proper ambient values. On the other hand, l is not firmly defined, although a length of a few times the boundary-layer thickness is plausible. In addition, a sensitivity of aircraft performance to ϵ must be considered exceptional, at least for turbulent designs. Therefore, this line of reasoning still does not narrow the range of defendable values to less than several factors of 2. Accordingly, other criteria are sought later.

A separate argument is that the physical merit of any influence the ambient values have inside the boundary layers via the model's diffusion terms is very debatable. In fact, this influence has at times been deeply troublesome, in the cases of the pure $k-\omega$ model and of the Baldwin–Barth model (see Menter [8,9]). In short, a low sensitivity to the chosen values is desired. The situation in external aerodynamics is far removed from bypass transition.

A milder version of this *reinterpretation* of k and ϵ as not representing the totality of the turbulence occurs in the logarithmic layer. The two equations (1) and (2) demand a plateau with $k^+ = 1/\sqrt{C_\mu}$, yet the true TKE found from experiments and direct numerical simulation (DNS) is far from uniform, leading to the view that the modeled k represents only the *active* energy, which has length scales on the order of the wall distance and contributes to the shear stress. In that sense, it is also a high-pass-filtered version of the complete k . The description of the $k-\omega$ model by Wilcox [5] also hints at such a view (see also v'^2 in the v^2-f model [10]).

For the SST model, the addition of sustaining terms yields the following equations:

$$\frac{Dk}{Dt} = \mathcal{P} - \beta^* \omega k + \frac{\partial}{\partial x_j} \left[\left(v + \frac{\nu_t}{\sigma_k} \right) \frac{\partial k}{\partial x_j} \right] + \beta^* \omega_{\text{amb}} k_{\text{amb}} \quad (10)$$

$$\begin{aligned} \frac{D\omega}{Dt} = & \frac{\gamma}{\mu_t} \mathcal{P} - \beta \omega^2 + \frac{\partial}{\partial x_j} \left[\left(v + \frac{\nu_t}{\sigma_\omega} \right) \frac{\partial \omega}{\partial x_j} \right] \\ & + 2(1 - F_1) \frac{1}{\sigma_\omega^2 \omega} \frac{\partial k}{\partial x_j} \frac{\partial \omega}{\partial x_j} + \beta \omega_{\text{amb}}^2 \end{aligned} \quad (11)$$

In other words, the model is identical to the original SST model in every respect except for the addition of constant sustaining terms $\beta^* \omega_{\text{amb}} k_{\text{amb}}$ and $\beta \omega_{\text{amb}}^2$. In the freestream, these have the effect of exactly cancelling the destruction terms if $k = k_{\text{amb}}$ and $\omega = \omega_{\text{amb}}$. Inside the boundary layer, they are generally orders of magnitude smaller than the destruction terms for reasonable freestream turbulence levels (say, $Tu = 1\%$ or less) and therefore have little effect. At first sight, setting ambient values adds to the user's burden; but in fact, these levels can be identical to the inflow values. Furthermore, they can be recognized in the near field and sensibly compared with the values that prevail in the turbulent regions. Thus, the situation is markedly simplified, and this option is both practical

[‡]Private communication with R. Langtry.

and good for user awareness. We can now turn to the choice of these ambient values.

III. Ambient Values

Turbulence modeling is a pragmatic endeavor, and we are seeking *effective* values in the sense outlined already, without precise reference to *true* measurable levels of k and ε , let alone ν_t . We also consider the common situation in which the ambient values are picked to trigger turbulence in all boundary layers without local tripping, except perhaps at very low Reynolds numbers. Before making our recommendations, we review the possible bases for picking ambient values.

A. Turbulent Reynolds Number

It is natural to compare the eddy viscosity ν_t to the molecular viscosity ν , but serious misconceptions have ensued. First, the idea that outside of the boundary layers, it must satisfy $\nu_t/\nu \ll 1$, because *there is no turbulence*, is erroneous, as will be shown. Values much higher than this remain effective when the flow Reynolds number is high enough (unless, of course, laminar boundary layers are desired). Second, objections to very high values of ν_t/ν are also erroneous and have caused trouble in at least one code. The ratio ν_t/ν had been limited to 10^5 (at first sight, a very large number) in response to some convergence troubles; however, 10^5 is routinely exceeded in jets at full-scale aerospace Reynolds numbers. Any such hard-wired limiters should be removed from all codes. They create a Reynolds-number dependence that runs completely against turbulence theory in free shear flows. This also applies to adjustable limiters offered to users in some codes. In some situations, RANS models err by having too high an eddy viscosity; examples include free vortices for most models and fully developed round jets for the S-A model. A more accurate solution can then be obtained by manually lowering the eddy viscosity, and some users experiment (say, with a limit such as $\tilde{\nu}/\nu \leq 10^4$). The danger is that in free shear flows, this limiter should scale proportionally to the flow Reynolds number, and the user's manuals give no guidance on this. Massive inaccuracies can again result at full-size Reynolds numbers.

The area in which ν_t/ν has control and is meaningfully compared with unity concerns transition in the S-A model. Ambient values of $\tilde{\nu}/\nu$ well below 1, such as 0.1, will cause the model to remain dormant. Values well above 1, such as 3, will cause it to grow turbulent in all boundary layers at reasonably high Reynolds numbers. This is by design. There is no reason to pick values much above 3, even when fully turbulent behavior is desired. This will ensure that ambient values do not influence the interior of the

boundary layer, except for steering it toward laminar or turbulent levels, which is binary.

B. Boundary-Layer Levels and Device Reynolds Numbers

If the ambient values, which have been seen to be quite arbitrary, are not to influence the boundary layer through diffusion, then these values need to be decidedly lower than values in the boundary-layer's outer region. These are on the order of $10^{-3}U^2$ for k , where U is a typical edge velocity, and $10^{-4}U^3/\delta$ for ε , where δ is the boundary-layer thickness; finally, using the standard formulas and because C_μ is close to 0.1, ω is simply on the order of U/δ , and ν_t on the order of $10^{-3}U\delta$. It must be remembered that ν_t itself is not diffusing in two-equation models, and its ambient value is not directly relevant: the k - ε equations tend to draw ν_t down near the boundary-layer edge [11]. However, removing the decay of the primary variables via floor values or sustaining terms also sets ν_t .

An example of the corruption of the solution in the boundary layer by high ambient turbulence is shown in Fig. 2. Here, the floor value for k/U^2 is 1.5×10^{-6} , and the floor value for $\omega L/U$ is varied. When it is very high (over 1000), the natural decrease of ω away from the wall is interrupted only one-third of the way up the boundary layer, and the velocity profile is damaged as a result. This illustrates a danger of the practice of removing free decay of turbulence: recall that with free decay over a distance of $50L$, $\omega L/U$ could not exceed 0.24. This figure, incidentally, confirms the estimate of U/δ for the outer-layer levels of ω . Also note the large dynamic range of ω , and therefore ε , within a boundary layer; wall values would not be relevant in this context.

Another very concrete consideration in aerospace applications is the gap regions between different elements of a wing. These are normally designed to allow a potential core between the two boundary layers. It is all too easy to set the ambient ν_t so high that this potential core is smeared and to remain unaware of this fact, deeply hidden in the flowfield. This can be a major source of inaccuracies in CFD and of sensitivity to ambient values. The gap d is often on the order of 1% of the chord, and the gap/eddy-viscosity Reynolds number dU/ν_t must be in excess of about 100, and therefore the chord/eddy-viscosity Reynolds number must be in excess of 10^4 . Even single-element wings have small features for which the potential flow should not be corrupted; the leading-edge radius is a few percent of the chord. Again, only extensive examinations of the flowfield would reveal such violations, and so it is highly desirable to prevent them from ever occurring in the first place by good standard practices. Normally, the constraint for the eddy viscosity to be dominated by the boundary-layer eddy viscosity $\nu_t < 10^{-3}U\delta$ is stronger than the gap constraint $\nu_t \ll Ud$, but both should be kept in mind.

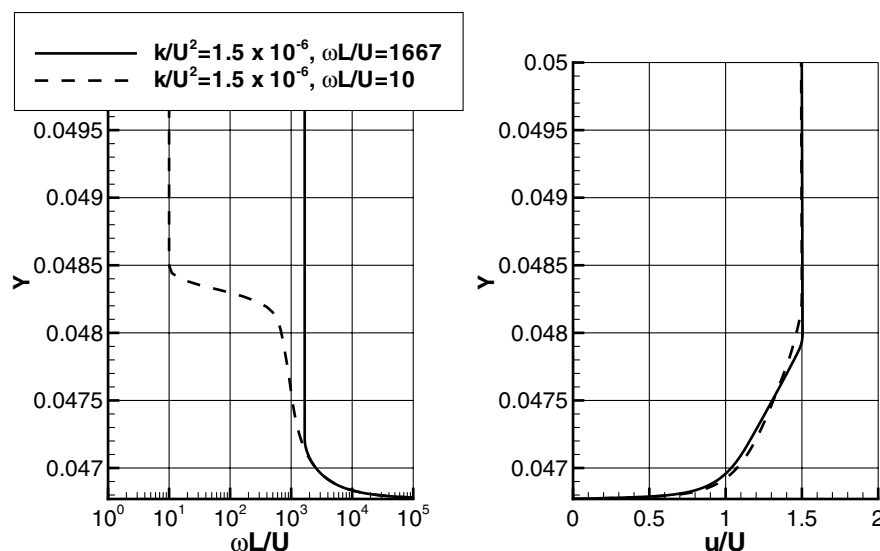


Fig. 2 Effect of ambient ω on the boundary layer of a NACA 0012 airfoil with $Re_c = 10^7$.

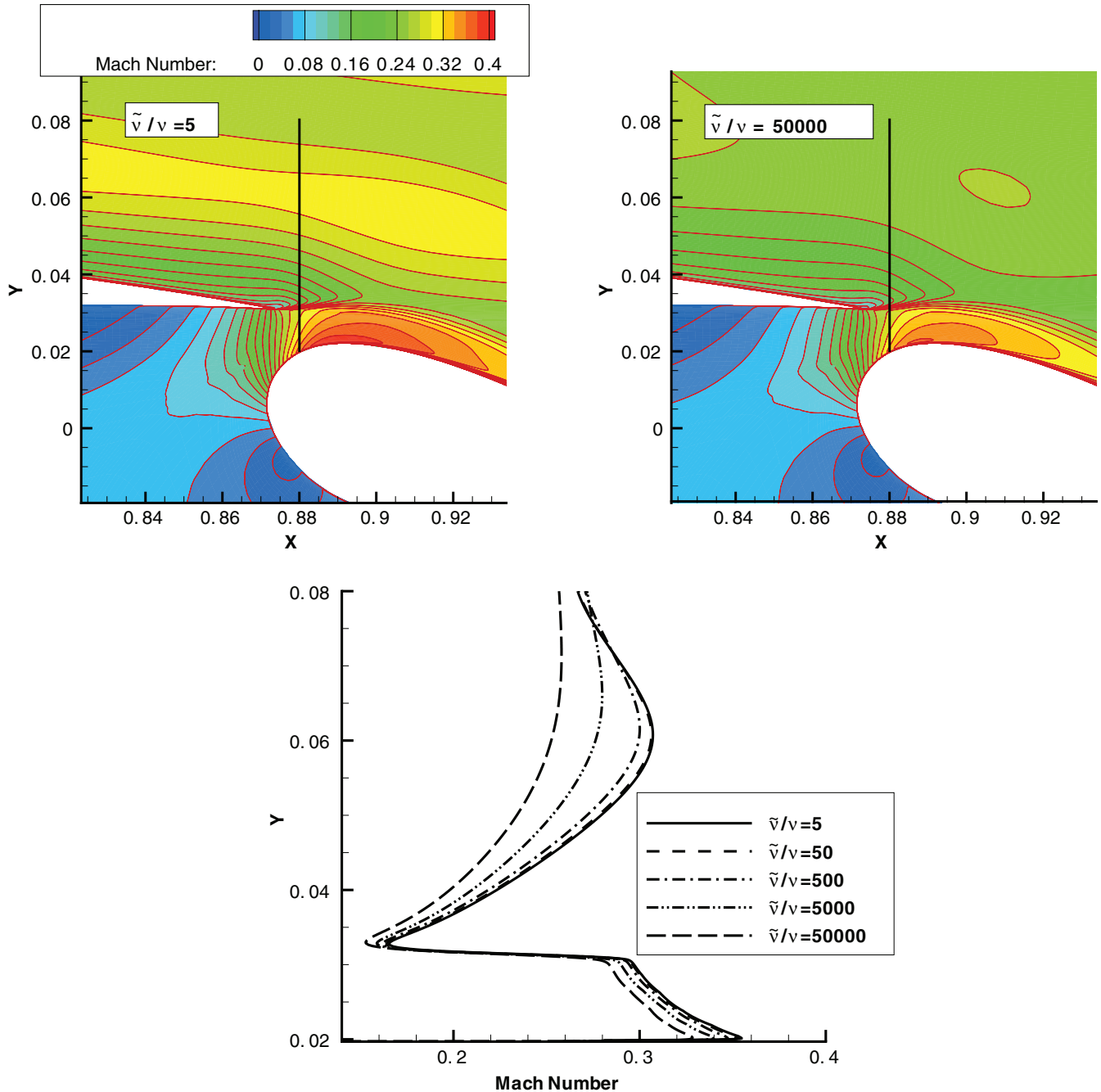


Fig. 3 Multi-element airfoil flowfields using S-A ($M = 0.2$ and $Re_c = 9 \times 10^6$) showing a) Mach contours near the flap gap for $\tilde{v}/v = 5$, b) Mach contours near the flap gap for $\tilde{v}/v = 50000$, and c) profiles of the Mach number along $x/c = 0.88$ for $\tilde{v}/v = 5$ to 5000 in factors of 10.

Figure 3 shows solutions of a multi-element airfoil at $Re_c = 9 \times 10^6$, with the S-A model and different ambient turbulence levels. As \tilde{v}/v is increased, the contamination in the solution gets progressively worse; note, however, that the solution degradation only starts to become noticeable at very high levels, greater than 500 or so (the low ambient value of $\tilde{v}/v = 5$ is close to the recommended value of 3 and could be considered as standard). In other words, the acceptable range for \tilde{v}/v is very wide. However, note that this range shrinks with lower Reynolds numbers.

Figure 4 displays the eddy viscosity, comparing a standard ambient value of $\tilde{v}_{FS}/v = 5$ with a high value of $\tilde{v}_{FS}/v = 5000$. Using the ambient turbulent value of 5 makes \tilde{v}/v visible on a scale of hundreds only in the free shear layers and clearly originating near the walls. In contrast, the solution with excessive ambient \tilde{v} has a high plateau away from the airfoil. The S-A destruction term activates in response to the high plateau level and strongly reduces \tilde{v}/v , from 5000 gradually toward 0 near the wall. It is still excessive, of course,

and the eddy-viscosity fields are grossly different, particularly in the free shear layers. The approximate destruction equation is $u \cdot \nabla(1/\tilde{v}) = 2c_{w1}/d^2$, where d is the distance to the wall (because in irrotational regions $r \gg 1$, so that $f_w = c_{w3} = 2$). For a streamline directly approaching the airfoil without deceleration, its solution is

$$\frac{1}{\tilde{v}} = \frac{1}{\tilde{v}_{FS}} + \frac{2c_{w1}}{Ud} \quad (12)$$

which limits \tilde{v} from above with $Ud/2c_{w1}$ (recall that $c_{w1} = 3.2$). This explains why the plateau at $\tilde{v} = 5.5 \times 10^{-4}UL$ starts dropping near $d = 0.05$, ahead of the slat, in Fig. 4b. The drop is then faster than in Eq. (12), because the local velocity u is rapidly dropping below U . For streamlines that flow past the airfoil, the velocity is closer to U , but the destruction effect is cumulative, and a kind of superboundary layer forms. For a gap flow that would be entered by fluid *without* deceleration, the rough upper bound $Ud/2c_{w1}$ gives a gap Reynolds

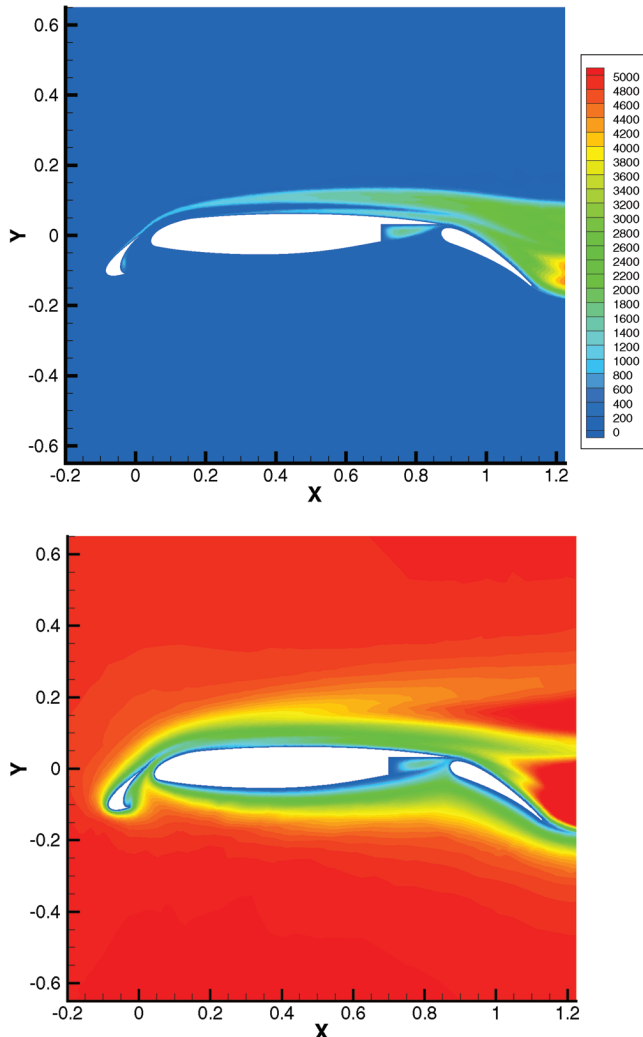


Fig. 4 Multi-element eddy-viscosity fields v_t/v using S-A ($M = 0.2$ and $Re_c = 9 \times 10^6$) showing a) inflow value $\tilde{v}_{FS}/v = 5$ and b) inflow value $\tilde{v}_{FS}/v = 5000$. Courtesy S. Allmaras.

number no lower than $4c_{w1}$, or 12.8; typically, it is well above 12.8, thanks to destruction accumulated along the airfoil. In Fig. 4b, the eddy viscosity in the flap gap does not exceed $\tilde{v}/v = 750$ (compare with $\tilde{v}_{FS}/v = 5000$ and $Ud/2c_{w1}/v \approx 7000$). The gap Reynolds number is about 180. With the normal inflow value in Fig. 4a, the gap Reynolds number is just 375 if based on the peak eddy viscosity, which propagates from the recirculation region in the flap cove. These two gap values for the different ambient levels are not hugely different, showing how the S-A model corrected the excessive inflow value to a good extent, for the gap. It also did rather well for the stagnation point. These are favorable consequences of a term that was calibrated for destruction in the logarithmic layer. However, the destruction term offers the free shear layers little protection: the peak eddy viscosity in the slat wake is artificially raised from about 2000 to 3000 when freestream \tilde{v}_{FS}/v goes from 5 to 5000.

Figure 5 illustrates the end effect of the variations on the lift coefficient. Again, \tilde{v}/v needs to reach 500, or about $Re_c/2 \times 10^4$, before the effect on lift is appreciable (3% with $\tilde{v}/v = 500$ and 12% with $\tilde{v}/v = 5000$). The estimate given earlier about $Re_c/10^4$ was therefore quite close.

Turning our attention to the leading edge, we find that the values of δ/L are quite Reynolds-number-dependent, because the laminar thickness is on the order of $\sqrt{vr/U}$ (with r being the leading-edge radius) and the turbulent thickness is often not much larger. However, the constraint on ε or ω will be more severe if based on the thicker regions, where δ is a few percent of chord. Free shear regions such as the slat wake have similar if not larger thicknesses

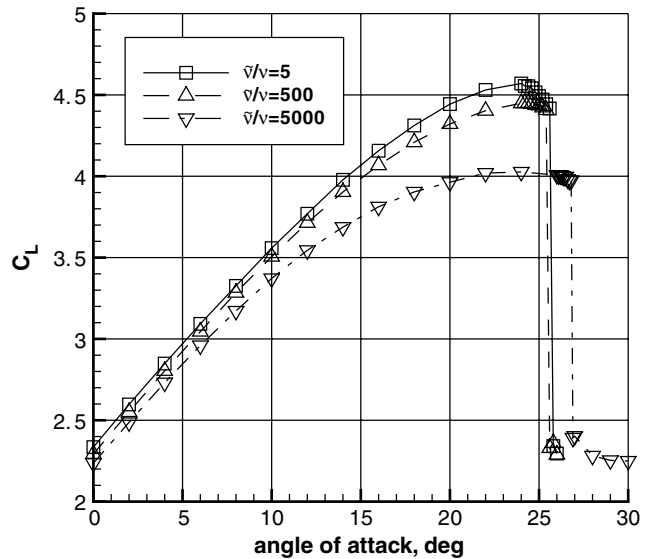


Fig. 5 Lift coefficient of the McDonnell-Douglas three-element airfoil with a range of values for ambient eddy viscosity; chord Reynolds number 9×10^6 ; courtesy of S. Allmaras.

and smaller velocity differences, which weakens their resistance. The merger of the slat wake with the main-element wake has a sizeable influence on the flow at some angles of attack, and therefore this wake cannot be sacrificed. This is not to imply that any of the present models approach perfection in predicting this merger, only that the solutions should be consistent between different codes and users.

C. Recommended Values

The preceding considerations lead to going-in upper bounds for the ambient primary-variable values $k \approx 1 \times 10^{-4} U^2$, $\varepsilon \approx 4.5 \times 10^{-5} U^3/c$, and $\omega \approx 5U/c$ (ε is derived from the other two, for which round numbers were picked). Here, $c = L$ is the airfoil chord. Use of these upper bounds implies $v_t \approx 2 \times 10^{-5} Uc$, which is small enough for flap gaps and well-developed boundary layers, but possibly too large for the leading-edge boundary layers. This may not strongly influence the rest of the flow, because the acceleration weakens the memory of the boundary layer. Still, some applications such as laminar-flow control and icing are dependent on high accuracy in the leading-edge region. This suggests lowering the allowable k to, say, $k \approx 1 \times 10^{-6} U^2$, while preserving $\omega \approx 5U/c$. This gives an upper bound on ε of $\approx 4.5 \times 10^{-7} U^3/c$, and $v_t \approx 2 \times 10^{-7} Uc$.

Note that this ambient value of ω (or $\varepsilon/C_\mu k$) is unreachable if free decay takes place. An accurate solution for free decay sets the value of k/ε in the neighborhood of $100c/U$ for a $50c$ domain, or $\omega \approx 0.1U/c$. Such a low value is not required by comparison with the boundary layer (Fig. 2) and is undesirable for the following reason: the SST model can encounter a particular problem when the ambient value of v_t/v is large and ω is set too small. The SST limiter chooses the maximum of $a_1\omega$ and ΩF_2 (Ω is the vorticity). Outside the boundary layer, $\Omega \rightarrow 0$ and $F_2 \rightarrow 0$, and it is the intention that the model choose $a_1\omega$ in this region. However, if ω is too small and residual vorticity is present, the two terms compete and the result can be an irregular eddy-viscosity distribution, as shown in Fig. 6. The main problem with this erratic behavior is that convergence can stall. Some implementations of the SST model use the strain rate instead of Ω , which is neutral in thin shear flows and helpful in this region, but this is not the reference formula. In our tests with the NACA 0012 airfoil, values of $v_t/v > 1$ and $\omega c/U < 3$ or so caused such problems (very high v_t/v levels on the order of 1000 with even larger $\omega c/U$ also displayed erratic behavior). Floor or sustained values are quite helpful in dealing with this problem. Figure 3 suggests that values of $\omega c/U$ up to 100 would be safe, so that the usable range is not too narrow.

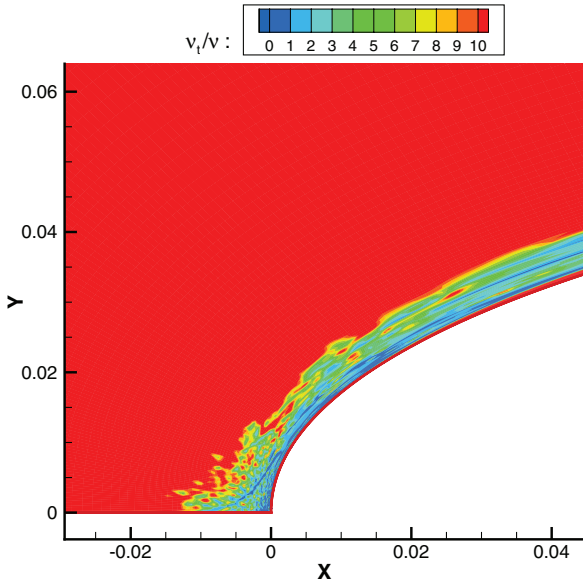


Fig. 6 Example of poor solution behavior of the SST model outside the boundary-layer edge, due to too-low ambient $\omega L/U = 0.2$; $v_t/v = 12.5$, NACA 0012 airfoil, $\alpha = 0$ deg, and $Re_c = 10^7$.

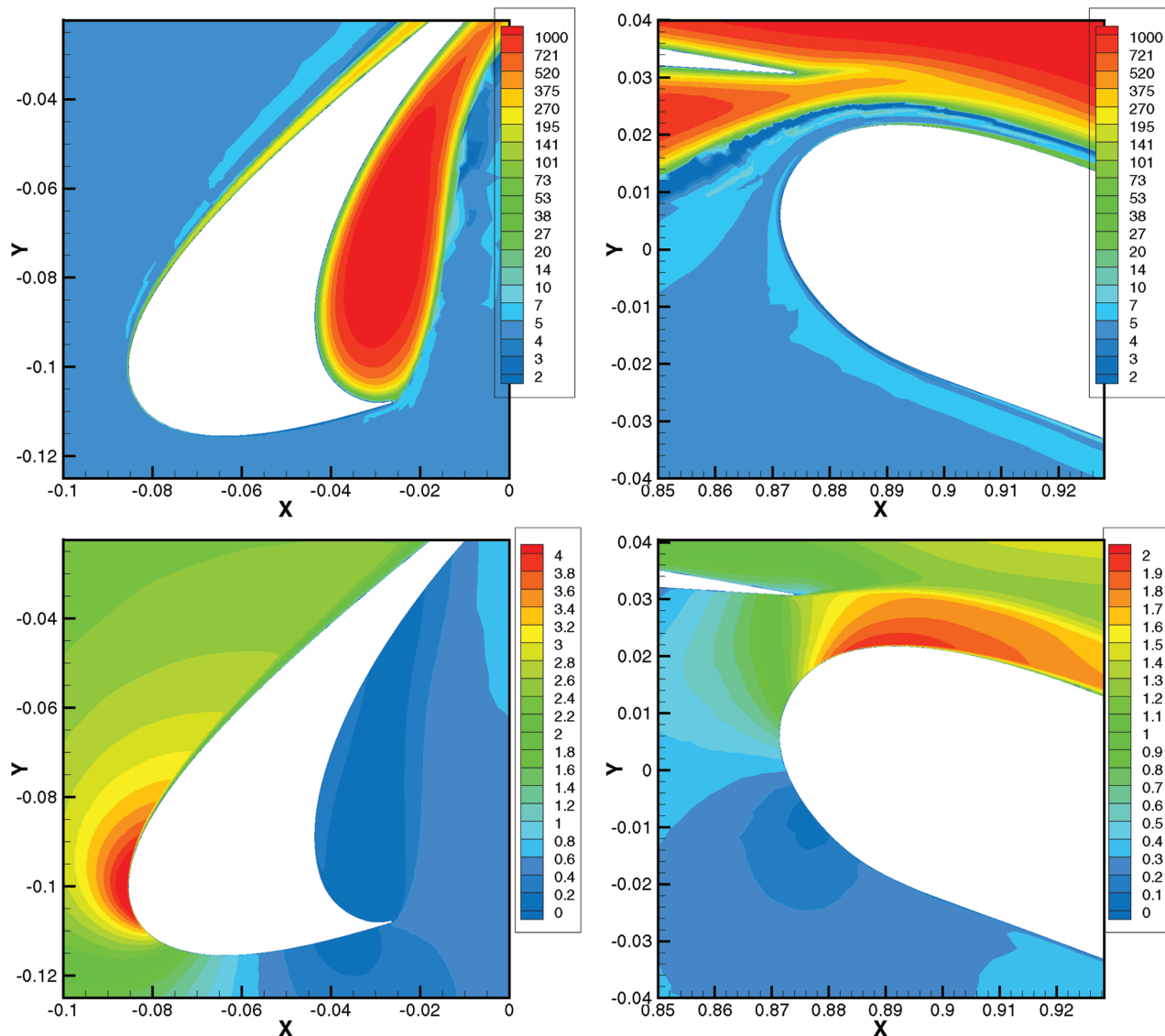


Fig. 7 Detail of the S-A solution of the McDonnell-Douglas three-element airfoil; upper frames: eddy viscosity and lower frames: velocity magnitude; chord Reynolds number 9×10^6 , $\alpha = 24$ deg, and $\tilde{v}_{FS}/v = 5$; unstructured grid, courtesy of S. Allmaras.

To summarize, the following ambient freestream turbulence values (in the region near the body) are recommended for general use for most typical external aerodynamic applications with two-equation turbulence models:

$$\frac{k}{U^2} = 1 \times 10^{-6} \quad (13)$$

$$\frac{\varepsilon c}{U^3} = 4.5 \times 10^{-7} \quad (14)$$

$$\frac{\omega c}{U} = 5 \quad (15)$$

This recommended level of k gives a Tu near $\approx 0.08\%$, and all the values yield an ambient eddy-viscosity ratio of $v_t/v \approx 2 \times 10^{-7} \times Re_c$. Thus, for example, for $Re_c = 10 \times 10^6$, $v_t/v \approx 2$, and $Re_c = 10^6$, $v_t/v \approx 0.2$. Again, these ambient levels are not achievable if the turbulence variables are allowed to decay naturally according to the turbulence equations. One easy way to achieve these ambient levels in practice is to choose them as both inflow and floor (sustained) values through the addition of sustaining terms such as those given in Eqs. (10) and (11).

For S-A, the values $\tilde{v}/v = 3-5$ are well-placed for fully turbulent behavior, with 3 being somewhat preferable at the lowest Reynolds numbers, because it gives $v_t/v \approx 0.2$, well below 1. Higher values

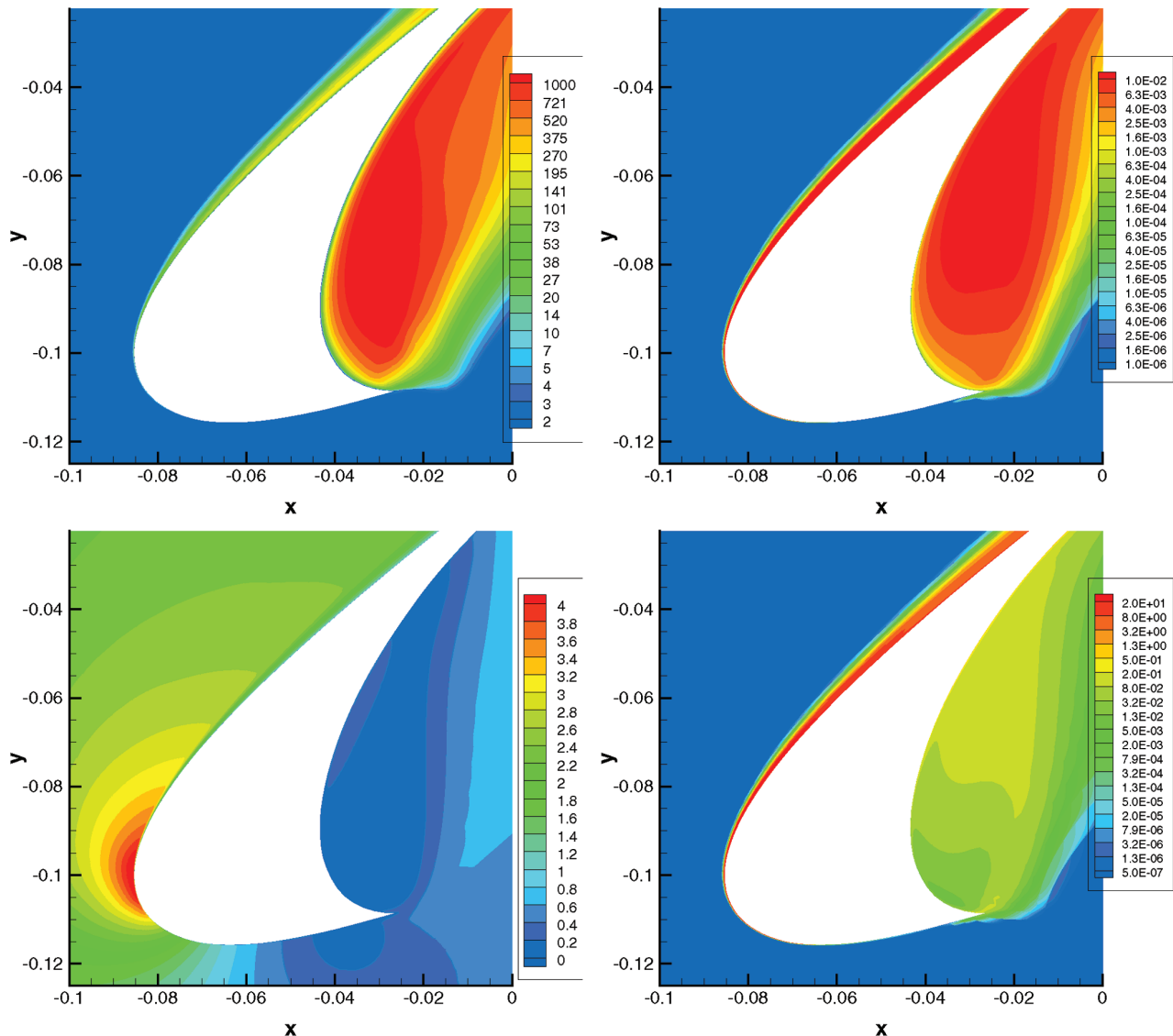


Fig. 8 Detail of the SST solution of the McDonnell–Douglas three-element airfoil; upper left: eddy viscosity v_t/v , upper right: k/U^2 , lower left: velocity magnitude, and lower right: ω_c/U ; $Re_c = 9 \times 10^6$, $\alpha = 19$ deg, $k_{FS}/U^2 = 1 \times 10^{-6}$, and $\omega_{FS}/U = 5$, with sustaining terms.

may slightly help convergence at high Reynolds numbers by smoothing out the edges of turbulent regions, but not enough to motivate giving up the simple recommendation.

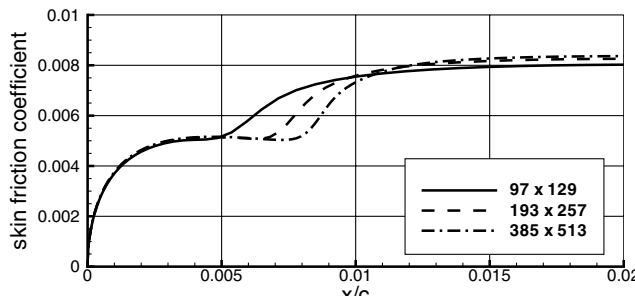
Figure 7 explores the S–A flowfield for a multi-element configuration using $\tilde{v}_{FS}/v = 5$, with emphasis on the stagnation regions. An exponential scale is used in this figure for eddy viscosity. It is quite smooth on this grid, although with a little noise in the 5–10 range. Although not shown, a computation on a coarser grid (about one-fourth of the number of points) was not smooth for the low values of \tilde{v} up to about 50, and it also had significant negative excursions of \tilde{v} in the flap gap, traced to irregularities in the adaptive unstructured grid. The fine grid has negative values only very far downstream (and in this code, when $\tilde{v} < 0$, v_t is set to 0). Multiblock structured grids generate their own disruptions, but they appear to be milder and confined to block corners and small regions with highly stretched and distorted cells. There is no evidence here that the imperfect solution is harming the physics of the model, but a blanket statement can certainly not be made. For instance, contact between unphysical hot spots and the flap upper-surface boundary layer could precipitate transition in a grid-dependent manner.

Also striking in this computation is the fact that the model does not depart from laminar for quite some distance in some of the boundary layers. For instance, the lower stagnation point on the slat is near $x = -0.035$, and appreciable eddy viscosity does not grow until the adverse pressure gradient at $x = -0.085$. This supports an earlier

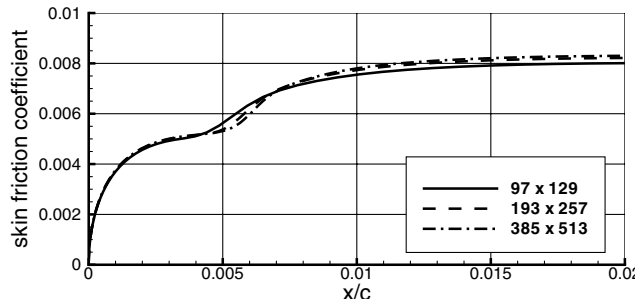
comment about the boundary-layer thicknesses in laminar and turbulent flow in stagnation regions being close (even at a high chord Reynolds number). The boundary layer is vigorously thinned out by the acceleration, yet the model remains poised to grow turbulent values, because the ambient value was chosen for that. The flap lower-surface boundary layer, similarly, is free of significant turbulence within the frame shown; it grows very gradually, to reach 27 at the trailing edge. The turbulence index i_t (S–A [2]) is about 0.5 at the stagnation points, but rises to 1 rapidly. Note, however, that this behavior is much more marked in 2-D flows than in general.

Figure 8 is a similar figure for the SST model; the left two frames can be directly compared with those in Fig. 7. The three turbulence variables are shown in exponential scales again, with the darkest blue for the ambient values. The recommended ambient values (also used as sustained values) appear very effective, in that they are smaller than the boundary-layer values almost everywhere along the wall, yet transition is occurring reliably. Note mild differences between the S–A and SST models in the slat cove: the peak eddy-viscosity values are 1650 and 1800, respectively, and the SST recirculation bubble is accordingly wider. Conversely, the slat-upper-surface boundary layer near $x = -0.025$, S–A peaks at 314, SST peaks at 277, and the S–A boundary layer is marginally thicker. Similar runs with the chord Reynolds number ranging from 10^6 to 10^8 were all successful.

Finally, Fig. 9 demonstrates how use of the recommended ambient values in the SST model can reduce the grid dependence of apparent



a) $k/U^2=1 \times 10^{-7}$, $\omega L/U=111.1$, no sustaining terms



b) $k/U^2=1 \times 10^{-6}$, $\omega L/U=5$, sustaining terms included

Fig. 9 Skin friction coefficient near the leading edge of the NACA 0012 airfoil at $Re_c = 10^7$ with the SST model; a) grid-dependent solution from Rumsey [1] using typical freestream turbulence levels and no sustaining terms; b) solution using recommended freestream turbulence levels with sustaining terms.

transition location for an airfoil computation. In Rumsey [1], the grid dependence was first demonstrated for typically used freestream turbulence levels, but a satisfactory explanation and cure were not found. Figure 9a shows the sort of grid-dependent transition seen. Although relatively small, this grid dependence could conceivably impact conclusions drawn from grid sensitivity studies, for example. In Fig. 9b, we find that by applying the currently recommended freestream levels and limiting via sustaining-term values (at the same levels), the grid dependence in transition location is largely eliminated.

IV. Conclusions

Inflow conditions for CFD with simple turbulence models in large domains were studied from theoretical and pragmatic points of view, with the following outcomes:

- 1) Simplistic and even erroneous conceptions in the community were discussed.
- 2) Rates of free decay for widely used two-equation model inflow levels were shown to be underresolved on typical far-field grids.
- 3) Excessively high values of eddy viscosity were demonstrated to contaminate the flowfield in nonturbulent regions.
- 4) The use of ambient values sustained by source terms in Eqs. (10) and (11) was advocated in two-equation models, whereas imposing floor values appeared to be a second-best solution.
- 5) Rational lower and upper bounds for these ambient values were provided.
- 6) Specific ambient turbulence values were recommended as safe starting points, located within rather wide intervals of low sensitivity.

The practice of arresting the decay, which conflicts with the two fundamental turbulence equations, was supported by theoretical considerations on the relevant range of turbulent motions. Thanks to having a single equation, the Spalart–Allmaras model readily provides an equivalent level of control, plus the ability to steer the boundary layers to be laminar or turbulent, without any special measures. If accepted, it is hoped that the present recommendations will spread in CFD codes after painless modifications, lowering the user's burden and rework, improving convergence and consistency between different users, and improving the accuracy of CFD solutions by removing unseen contaminations and helping users employ the models precisely as their authors intended.

This study emphasized numerical quality, convenience, and consistency in the context of everywhere-turbulent RANS calculations. Although a sizable range of ambient values was shown to work, it is still incumbent on users to justify to themselves the values they use and to run a few sensitivity checks. More refined practices that include laminar regions will require substantial improvements in the models and/or the discretizations, even outside the problem of predicting natural transition.

Acknowledgments

The authors thank M. Strelets and R. Langtry for valuable discussions and S. Allmaras for supporting calculations and discussions. The reviewers made excellent suggestions.

References

- [1] Rumsey, C. L., "Apparent Transition Behavior of Widely Used Turbulence Models," *International Journal of Heat and Fluid Flow* (to be published); also AIAA Paper 2006-3906, June 2006.
- [2] Spalart, P. R., and Allmaras, S. R., "A One-Equation Turbulence Model for Aerodynamic Flows," *La Recherche Aerospatiale: Bulletin Bimestriel de l'Office National d'Etudes et de Recherches Aerospatiales*, No. 1, 1994, pp. 5–21; also AIAA Paper 92-0439, Jan. 1992.
- [3] Goldberg, U., Peroomian, O., Chakravarthy, S., and Sekar, B., "Validation of CFD++ Code Capability for Supersonic Combuster Flowfields," AIAA Paper 97-3271, 1997.
- [4] Menter, F. R., "Two-Equation Eddy-Viscosity Turbulence Models for Engineering Applications," *AIAA Journal*, Vol. 32, No. 8, 1994, pp. 1598–1605.
- [5] Wilcox, D. C., *Turbulence Modeling for CFD*, 3rd ed., DCW Industries, La Cañada, CA, 2006.
- [6] Baldwin, B. S., and Barth, T. J., "A One-Equation Turbulence Transport Model for High Reynolds Number Wall-Bounded Flows," NASA TM-102847, Aug. 1990.
- [7] Abdol-Hamid, K. S., Lakshmanan, B., and Carlson, J. R., "Application of Navier–Stokes Code PAB3D with $k-\epsilon$ Turbulence Model to Attached and Separated Flows," NASA TP-3480, Jan. 1995.
- [8] Menter, F. R., "Influence of Freestream Values on $k-\omega$ Turbulence Model Predictions," *AIAA Journal*, Vol. 30, No. 6, 1992, pp. 1657–1659.
- [9] Menter, F. R., "Eddy Viscosity Transport Equations and Their Relation to the $k-\epsilon$ Model," *Journal of Fluids Engineering*, Vol. 119, No. 12, 1997, pp. 876–884.
- [10] Kaltzen, G., "Application of the $v^2 - f$ Turbulence Model to Transonic Flows," AIAA Paper 99-3780, June–July 1999.
- [11] Cazabou, J. B., Spalart, P. R., and Bradshaw, P., "On the Behavior of Two-Equation Models at the Edge of a Turbulent Region," *Physics of Fluids. A*, Vol. 6, No. 5, 1994, pp. 1797–1804.

P. Givi
Associate Editor